Effects of Diabetes and Gender on Mechanical Properties of the Arterial System in Rats: Aortic Impedance Analysis[1]

KUO-CHU CHANG,[2]* KWAN-LIH HSU,† AND YUNG-ZU TSENG*†

*Department of Physiology, College of Medicine, National Taiwan University, Taipei, Taiwan; and †Internal Medicine, National Taiwan University Hospital, Taipei, Taiwan

We determined the effects of diabetes and gender on the physical properties of the vasculature in streptozotocin (STZ)-treated rats based on the aortic input impedance analysis. Rats given STZ 65 mg/kg i.v. were compared with untreated age-matched controls. Pulsatile aortic pressure and flow signals were measured and were then subjected to Fourier transformation for the analysis of aortic input impedance. Wave transit time was determined using the impulse response function of the filtered aortic input impedance spectra. Male but not female diabetic rats exhibited an increase in cardiac output in the absence of any significant changes in arterial blood pressure, resulting in a decline in total peripheral resistance. However, in each gender group, diabetes contributed to an increase in wave reflection factor, from 0.47 ± 0.04 to 0.84 ± 0.03 in males and from 0.46 ± 0.03 to 0.81 ± 0.03 in females. Diabetic rats had reduced wave transit time, at 18.82 ± 0.60 vs 21.34 ± 0.51 msec in males and at 19.63 ± 0.37 vs 22.74 ± 0.57 msec in females. Changes in wave transit time and reflection factor indicate that diabetes can modify the timing and magnitude of the wave reflection in the rat arterial system. Meanwhile, diabetes produced a fall in aortic characteristic impedance from 0.023 ± 0.002 to 0.009 ± 0.001 mmHg/min/kg/ml in males and from 0.028 ± 0.002 to 0.014 ± 0.001 mmHg/min/kg/ml in females. With unaltered aortic pressure, both the diminished aortic characteristic impedance and wave transit time suggest that the muscle inactivation in diabetes may occur in aortas and large arteries and may cause a detriment to the aortic distensibility in rats with either sex. We conclude that only rats with male gender diabetes produce a detriment to the physical properties of the resistance arterioles. In spite of male or female gender, diabetes decreases the aortic distensibility and impairs the wave reflection phenomenon in the rat arterial system. Exp Biol Med 228:70–78, 2003

Key words: streptozotocin-diabetic rats; aortic input impedance; aortic distensibility; pulse wave reflection

Hyperglycemia in diabetes has been identified as an independent risk factor for the development of cardiovascular disease, including macroangiopathy and microangiopathy (1). Diabetes mellitus (DM) may reduce gender-related differences in the prevalence of cardiovascular disease by fading the vascular protective effects afforded by estrogen in females (2, 3). Reportedly, diabetic arteries are associated with high glucose-induced vascular dysfunction in that the contractile function of the vascular smooth muscle cells is impaired in rats treated with streptozotocin (STZ) (4, 5). The contractile dysfunction of the STZ-diabetic arteries may result from changes in vasoactive substances and vasomotor responsiveness (6) and alterations in intracellular calcium handling (7). Such changes in cellular physiology of the diabetic arteries may cause a detriment to the mechanical properties of the arterial system in STZ-diabetic rats. Although the measurement on pulsatile pressure-flow relation of the arterial system has been made in male STZ-diabetic rats (5, 8, 9), little attention has been given to the role of gender in the modulation of diabetes-induced changes in blood flow as well as vascular dynamics.

To study a complete assessment of the physical properties of the arterial system, the technique of aortic input impedance analysis (10–12) has been used extensively in recent years (9, 13, 14). In the classic analysis of circulation, the arterial system is modeled as a steady-flow circuit in which the heart is represented by a steady-flow pump and the periphery by a simple resistance. In 1769, Stephen Hales likened the cushioning function of arteries to the action of a large distensible reservoir, which is referred to as Windkessel (10–12). The Windkessel represents the distensibility of the aorta and major arteries. Accurate characterization of the pulsatile component is important because it accounts for a substantial portion of the total load imposed on the left ventricle. In a pulsatile analysis of the cardiovascular sys-

[1] This study was supported by the National Taiwan University Hospital (grant NTUH92-5022).

[2] To whom requests for reprints should be addressed at Department of Physiology College of Medicine, National Taiwan University, No. 1, Section 1, Jen-Ai Road, Taipei, Taiwan. E-mail: kcchang@ha.mc.ntu.edu.tw

Received May 23, 2002.
Accepted August 21, 2002.

1535-3702/03/2281-0070$15.00

tem, the heart is represented by an intermittent source, and the vasculature may be modeled as a three-element Windkessel that consists of a series resistance (aortic characteristic impedance) and a parallel total peripheral resistance/total arterial compliance. Such an analysis of the arterial tree can be accomplished through the measurement of aortic input impedance that is the frequency relationship between the pressure and the flow signals measured in the ascending aorta.

The aortic input impedance embodies, in addition to vascular resistance (the nonpulsatile component of afterload), the summated effects of pulsatile component of afterload such as aortic stiffness and timing and magnitude of pulse wave reflection (10–12). In a hydraulic vascular system, the ratio of pulsatile pressure to flow is termed the aortic characteristic impedance (Z_c) if only centrifugal waves are present at origin. The aortic characteristic impedance is directly related to the blood density (ρ) and pulse wave velocity (c_0) and is inversely related to the lumen radius (r) squared of the tube: $Z_c = \rho c_0/\pi r^2$ (10–12). For large arteries, pulse wave velocity may be approximately related to the distensibility of the aortic wall (D): $c_0 = \sqrt{1/\rho D}$ where D refers to changes in volume (ΔV) in relation to changes in transmural pressure (ΔP), which is expressed as a fraction of the volume (V): $D = \Delta V/V\Delta P$. Meanwhile, compliance (C) is defined as a change in volume divided by a change in pressure ($C = \Delta V/\Delta P$) so that compliance equals distensibility times volume ($C = DV$) (15). As mentioned above, the aortic characteristic impedance has an inverse relation to the aortic distensibility so that Zc has been frequently used as an indicator of aortic stiffness: the higher the aortic characteristic impedance, the stiffer the aortic wall if aortic cross-sectional area remains unchanged. However, under certain circumstances, especially in rats with dilated aortic wall (9, 16), the aortic characteristic impedance probably could not describe the distensibility of aortas because of its inverse relation to aortic cross-sectional area. By contrast, being relatively independent to body shape, wave transit time (τ), which is inversely related to pulse wave velocity, could be derived to represent the distensibility of aortas in rats (9–12).

The wave transit time is the time for a wave to propagate from one end of the vasculature to the other. Because the aortic pressure wave can be regarded as a summation of its forward and backward components, the ratio of the backward pressure wave to the forward pressure wave is termed the wave reflection factor (R_f) (10–12). Therefore, both the wave transit time and the wave reflection factor may characterize the wave reflection phenomenon in the vasculature. The pulsatile hemodynamic parameters such as Z_c, τ, and R_f could be analyzed to delineate the pulsatile nature of blood flows in the arterial system. The static components of the arterial load such as mean aortic pressure as well as total peripheral resistance (R_p) can also be obtained from the measurement. The novelty of the aortic input impedance analysis is that one can distinguish the effects of diabetes and gender on Windkessel function from those on arteriolar function in rats treated with STZ.

The goal of the study was to determine the effects of diabetes and gender on the mechanical properties of the arterial system in STZ-treated rats based on the aortic input impedance analysis. The aortic input impedance spectra were obtained from the ratio of ascending aortic pressure harmonics to the corresponding flow harmonics using a standard Fourier series expansion technique (10–12). The aortic characteristic impedance was computed by averaging high-frequency moduli of the aortic input impedance data points (17,18). The wave transit time was determined by making use of the impulse response function of the filtered aortic impedance spectra (19).

Material and Methods

Experimental Preparations. Female or male Wistar rats weighing 220–260 g at the age of 2 months were used to induce DM in this study. Diabetes was induced by a single tail vein injection of STZ at a dose of 65 mg/kg (Sigma Chemical Co., St. Louis, MO). STZ was dissolved in 0.1*M* citrate buffer (pH 4.5). Control rats were given an intravenous injection of the vehicle. Forty-eight hours after the injection, induction of diabetes in the STZ-injected rat was confirmed by positive urine glucose using Ames Keto-Diastix (Miles Inc., Elkhart, IN). Studies on changes in arterial mechanics were performed 8 weeks after the induction of diabetes. All data collected from STZ-treated rats (male DM, $n = 12$; female DM, $n = 12$) were compared with those of untreated, age-matched controls (AC) (male AC, $n = 12$; female AC, $n = 12$). At the time of hemodynamic studies, arterial blood was collected for glucose measurement, and all female animals were at the stage of metestrus where most levels of female hormones are at their lowest levels. Rats were allowed free access to Purina chow and water and were housed two to three per cage in a 12:12-hr light:dark cycle animal room. The animal experiments were conducted according to the *Guide for the Care and Use of Laboratory Animals*, and were approved by the Animal Care and Use Committee of the National Taiwan University.

Catheterization. Each rat was intraperitoneally anesthetized with pentobarbital sodium (35 mg/kg). We monitored the animal's rectal temperature and used a heater to maintain the rat's body temperature. Tracheotomy was performed to provide artificial ventilation with a tidal volume of 5–6 ml/kg and respiratory rate of 50–70 breaths/min. The chest was opened through the second intercostal space of the right side. An electromagnetic flow probe (model 100 series, internal circumference 8 mm; Carolina Medical Electronics, King, NC) was positioned around the ascending aorta to measure the pulsatile aortic flow. A Millar catheter with a high-fidelity pressure sensor (model SPC 320, size 2F; Millar Instruments, Houston, TX) was used to measure the pulsatile aortic pressure. Before inserting, the pressure sensor was prewarmed in 37°C saline for at least 1 hr. The

catheter was inserted via the isolated right carotid artery into the ascending aorta. The catheter tip of the pressure transducer was positioned 1–2 mm distal to the downstream edge of the electromagnetic flow probe to avoid interference with the flow measurements. After being withdrawn from each rat, the catheter was reimmersed in the bath to check for baseline drift. At the end of the experiment, the pressure reading from the sensor submerged in the saline of less than 10 mm in depth was used as the zero pressure reference (13). The electrocardiogram (ECG) of lead II was recorded with a Gould ECG/Biotach amplifier (Gould Electronics, Cleveland, OH).

The analog waveforms were sampled at 500 Hz using a 12-bit simultaneously sampling analog-to-digital (A/D) converter (Acqutek Co., Taipei, Taiwan) interfaced to a personal computer. Selection of signals of 5–10 beats at steady state was made on the basis of the following criteria: recorded beats with optimal velocity profile that was characterized by a steady diastolic level, maximal systolic amplitude, and minimal late systolic negative flow; beats with an RR interval (cardiac cycle length) less than 5% different from the average value for all recorded beats; and exclusion of ectopic and postectopic beats. The selective beats were averaged in the time domain, using the peak R wave of ECG as a fiducial point. Timing between the pulsatile pressure and flow signals, due to spatial distance between the flow probe and proximal aortic pressure transducer, was corrected by a time-domain approach in which the foot of the pressure waveform was realigned with that of the flow (20). The resulting aortic pressure and flow signals were subjected to further impedance analysis.

Aortic Input Impedance Spectra. Aortic input impedance can be obtained from the ratio of ascending aortic pressure harmonics to the corresponding flow harmonics (Fig. 1, A and B) using a standard Fourier series expansion technique, shown in Appendix 1 (10–12). Herein, the flow meter (Model 501D; Carolina Medical Electronics) used has a frequency response that is decreased by 3 dB at approximately 100 Hz. The phase lag is almost linear with frequency (1.2 degrees/Hz). Corrections were performed to each impedance harmonic to take the phase delay into account. Total peripheral resistance of the systemic circulation (R_p) was calculated as mean aortic pressure divided by mean aortic flow. Aortic characteristic impedance of the systemic circulation (Z_c) was computed by averaging high-frequency moduli of the aortic input impedance data points (4th–10th harmonic) (17, 18). On the other hand, compliances corresponding to systolic, diastolic, and mean aortic pressure, respectively, could be obtained from the equation developed for an exponential pressure-volume relation, shown in Appendix 2 (21).

Vascular Impulse Response Function. The wave transit time (τ) could be determined by the impulse response function of the filtered aortic input impedance spectra (Fig. 1C). This was accomplished by inverse transformation of the aortic input impedance after multiplication of the first 12 harmonics by a Dolph-Chebychev weighting function with the order 24 (19). As is generally recognized, vascular reflections occur along the entire length of the arterial tree where a change in impedance exists (e.g., change in vessel diameter, wall stiffness, or vessel branching) (10–12). These multiple reflection sites contributes to diffuse reflections, which play an important role in wave dispersion. However, prior work by Westerhof's group (22) has demonstrated that the two reflection peaks usually seen in the canine vascular impulse response function represent pressure reflections from two effective reflection sites. The effective upper body site gives rise to the first reflection peak, and the lower body site gives rise to the second reflection peak. Because the apparent time of the first peak is heavily influenced by early diffuse reflections, one could take that of the second peak as the standard for the calculation of wave transit time in the lower body circulation, when the time of the initial peak is used as the reference (Fig. 1C) (23). Meanwhile, the time domain reflection factor (R_f) could be derived as the amplitude ratio of backward-to-forward peak pressure wave by the method Westerhof *et al.* (24) proposed, shown in Appendix 3. Therefore, both the wave transit time and the wave reflection factor may characterize the wave reflection phenomenon in the vasculature.

Statistics. Results are expressed as means ± SE. Because cardiac output is significantly related to body shape, this variable was normalized to body weight when comparison was made between STZ-diabetic rats and age-matched controls. Other hemodynamic variables derived from blood flow were also normalized to body weight to detect the effects of diabetes and gender on these parameters. A two-way analysis of variance (ANOVA) was used to determine the effects of diabetes on the physical properties of the vasculature in STZ-treated rats of either gender. Simple effect analysis was used when significant interaction between diabetes and gender occurred. Differences among means within levels of a factor were determined by Tukey's honestly significant difference (HSD). Significant differences were assumed at the level of $P < 0.05$.

Results

Table I shows the effects of diabetes and gender on body weight, blood glucose level, and arterial blood pressure. As expected, after the β-cells of the islets of Langerhans were destroyed by STZ, diabetic rats of either gender had higher blood glucose levels than did age-matched controls. Diabetes was associated with a decrease in body weight in both male and female STZ-treated rats. Neither diabetes nor gender produced a significant difference in aortic pressure profile, nor was there a diabetes × gender interaction for arterial blood pressure.

Figure 2 shows the effects of diabetes and gender on the basic hemodynamic data, including basal heart rate (HR), cardiac output (CO), stroke volume (SV), and total peripheral resistance (R_p). Both diabetes and female gender significantly lowered HR (Fig. 2A). However, no interaction

between the effects of diabetes and gender on HR was observed in rats. A significant interaction between the effects of diabetes and gender in their effects on CO (Fig. 2B), SV (Fig. 2C), and R_p (Fig. 2D) was detected. Although producing an increase in CO and a decrease in R_p in males, diabetes exhibited no significant changes in CO and R_p in females. Male STZ-diabetic rats had higher CO and lower R_p than did female STZ-diabetic rats. On the other hand, an interaction showed that diabetes significantly enhanced SV in rats with either gender, and male STZ-diabetic animals had higher SV than did female STZ-diabetic animals. Unlike rats with insulin deficiency, age-matched controls exhibited no significant changes with sex in HR, CO, SV, or R_p.

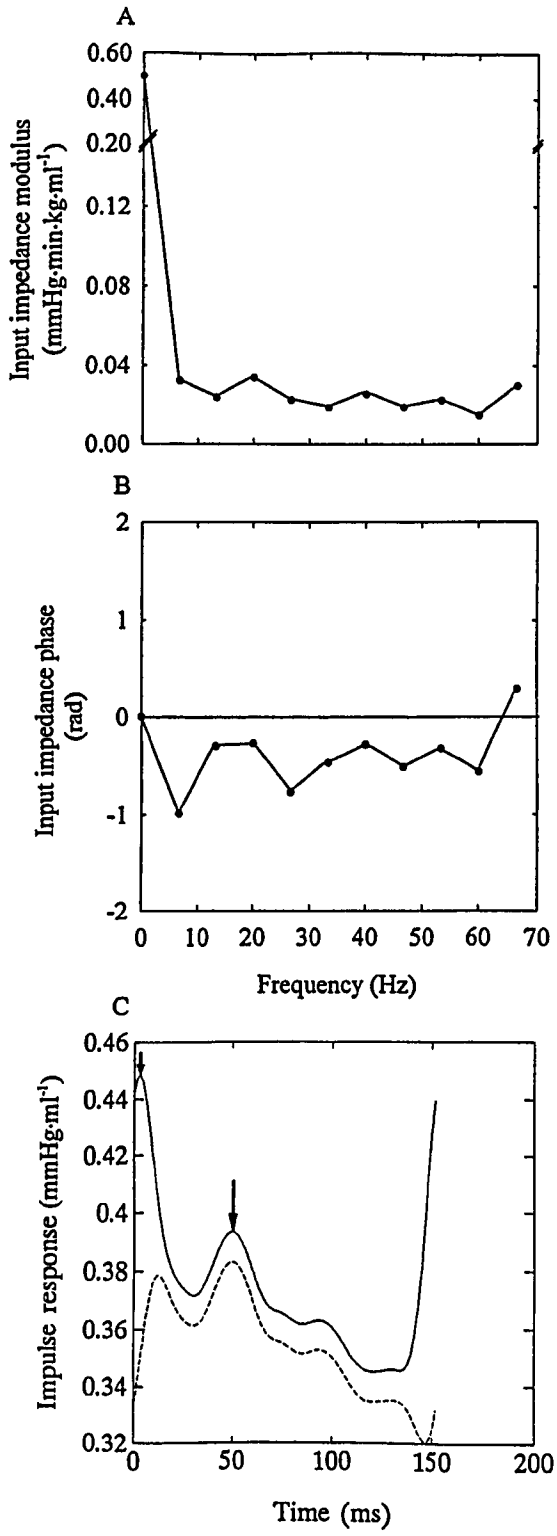

Figures 3 and 4 show the effects of diabetes and gender on the pulsatile nature of blood flows in arteries in terms of aortic characteristic impedance (Z_c), wave transit time (τ), and wave reflection factor (R_f). No interaction between the effects of diabetes and gender in their effects on Z_c was detected in rats (Fig. 3A). However, diabetic rats had decreased Z_c at 0.009 ± 0.001 vs 0.023 ± 0.002 mmHg/min/kg/ml in males and at 0.014 ± 0.001 vs 0.028 ± 0.002 mmHg/min/kg/ml in females. There was a significant interaction between the effects of diabetes and gender in their effects on aortic compliances (C_s in Fig. 3B, C_d in Fig. 3C, and C_m in Fig. 3D). Although producing an increase in aortic compliances in males, diabetes exerted no significant changes in aortic compliances in females. Male STZ-diabetic rats had higher aortic compliances than did female STZ-diabetic rats. Unlike rats with insulin deficiency, age-matched controls showed no significant changes with sex in Z_c, C_s, C_d, or C_m.

In each gender group, diabetes elicited a decline in the magnitude of the forward pressure (P_f in Fig. 4A), but had no effects on magnitude of the backward pressure (P_b in Fig. 4B), leading to an increase in R_f from 0.47 ± 0.04 to 0.84 ± 0.03 in males, and from 0.46 ± 0.03 to 0.81 ± 0.03 in females (Fig. 4C). Neither diabetes nor gender affected P_b, nor was there a diabetes × gender interaction for P_b. On the other hand, no interaction between the effects of diabetes and gender in their effects on τ was detected in the rats (Fig. 4D). However, diabetic rats had reduced τ at 18.82 ± 0.60 vs 21.34 ± 0.51 msec in males and at 19.63 ± 0.37 vs 22.74 ± 0.57 msec in females. Unlike STZ-diabetic rats, age-matched controls showed no significant changes with sex in wave reflection phenomena in terms of both the wave reflection factor and the wave transit time.

Discussion

The major findings of this study are that only in male rats does diabetes produce a detriment to the mechanical properties of the resistance arterioles. However, despite

Figure 1. Modulus (A) and phase (B) of the aortic input impedance, and impulse response function of the filtered impedance spectra (C) in one control rat with female gender. The aortic input impedance spectra were computed from the aortic pressure and flow signals using a standard Fourier series expansion technique shown in Appendix 1. In C, the dashed line indicates that the characteristic impedance component of the vascular impulse response has been removed. The long arrow shows the discrete reflection peak from the body circulation and the short arrow demonstrates the initial peak as a reference. In the solid line, one-half of the time difference between the appearance of the reflected peak (long arrow) and the initial peak (short arrow) approximates the wave transit time in the lower body circulation.

Table I. Effects of Diabetes and Gender on Body Weight, Blood Glucose Level, and Aortic Pressure Profile in Wistar Rats

	Males		Females	
	AC (n = 12)	DM (n = 12)	AC (n = 12)	DM (n = 12)
Body weight (g)	499.0 ± 14.1	236.4 ± 8.9[a]	296.5 ± 3.6[b]	241.0 ± 6.0[a]
Glucose (mg/dl)	113.0 ± 3.9	403.7 ± 10.4[a]	124.0 ± 6.0	420.3 ± 12.3[a]
P_s (mmHg)	133.2 ± 3.5	124.9 ± 3.1	129.4 ± 2.4	128.0 ± 2.5
P_d (mmHg)	103.2 ± 3.2	97.7 ± 2.8	96.8 ± 2.8	101.1 ± 2.3
P_m (mmHg)	118.4 ± 3.6	111.6 ± 2.8	113.8 ± 2.7	115.5 ± 2.2

Note. All values are expressed as means ± SE, P_s, systolic aortic pressure; P_d, diastolic aortic pressure; P_m, mean aortic pressure; AC, age-matched controls; DM, STZ-diabetic rats.
[a] Difference between STZ-diabetic rats and age-matched controls with either male or female gender ($P < 0.01$).
[b] Difference between males and females in age-matched controls ($P < 0.01$).

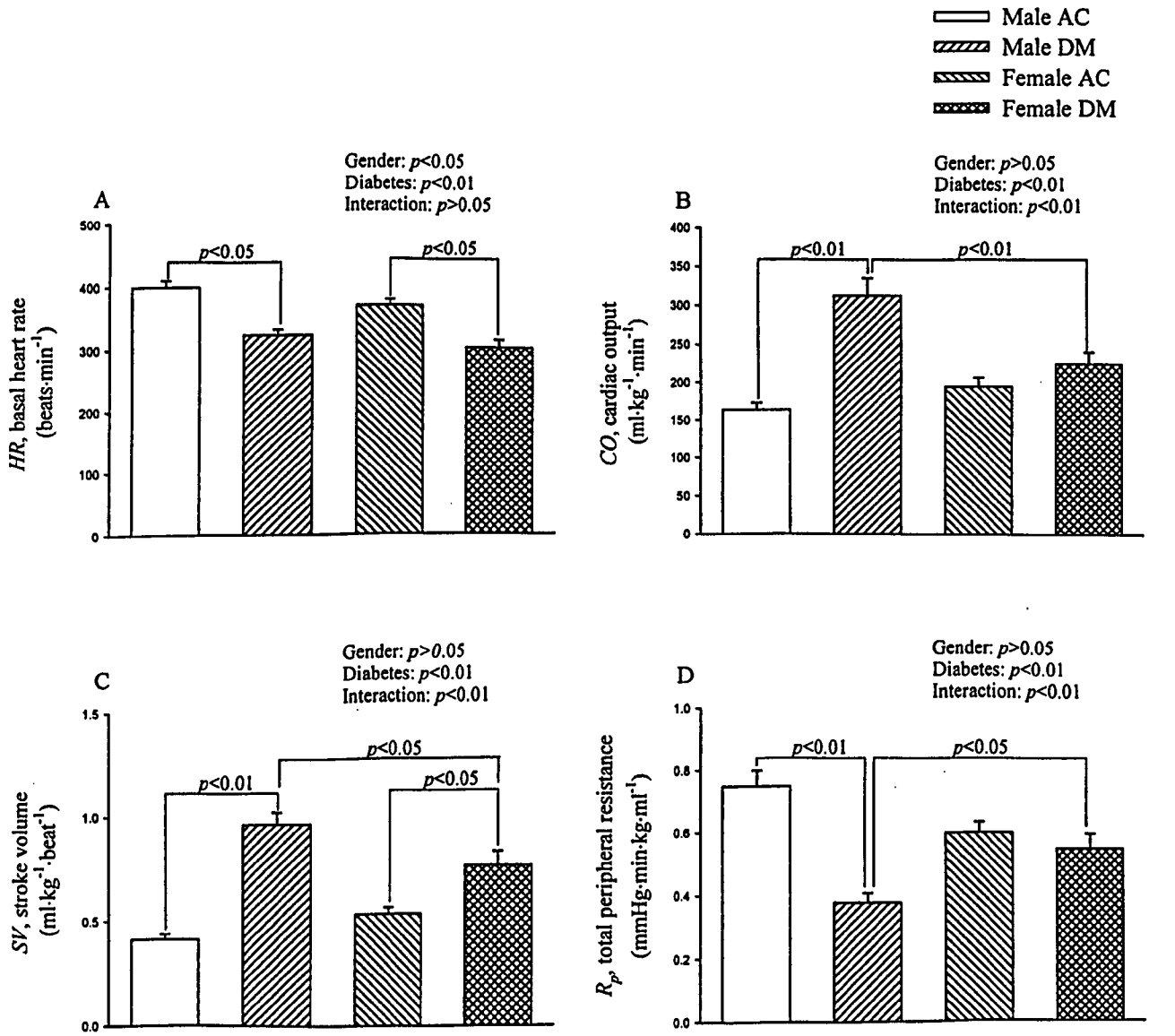

Figure 2. Effects of diabetes and gender on basal HR (A), CO (B), SV (C), and R_p (D). AC, age-matched controls; DM, STZ-diabetic rats.

gender, diabetes diminishes the aortic distensibility and impairs the wave reflection phenomena in the rat arterial system.

An increase in blood flow that occurs in the absence of any significant changes in arterial blood pressure is termed isobaric vasodilatation. Male but not female STZ-diabetic rats showed isobaric vasodilatation, resulting in a decrease in total peripheral resistance (R_p in Fig. 2D). With unchanged mean aortic pressure, a decline in total peripheral

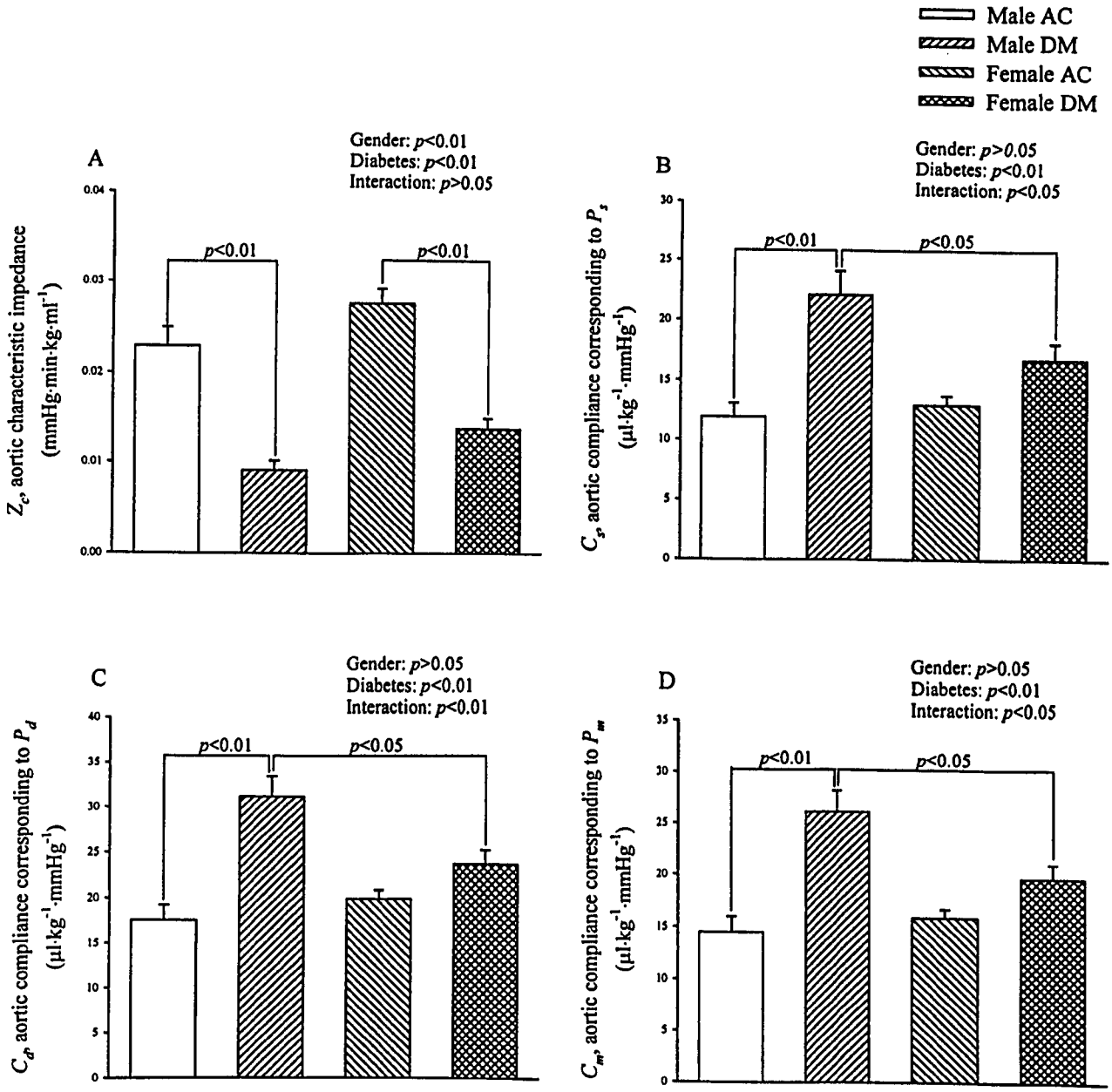

Figure 3. Effects of diabetes and gender on Z_c (A), C_s (B), C_d (C), and C_m (D). AC, age-matched controls; DM, STZ-diabetic rats.

resistance suggests that the contractile function of the vascular smooth muscle cells may be impaired in resistance arteriole (4). The contractile dysfunction of the vascular smooth muscle cells may cause a fall in vascular smooth muscle tone, which is responsible for an increase in arteriolar caliber. This suggests that capillary hypertension may occur in male STZ-diabetic rats while arterial blood pressure remains unchanged, developing diabetic vascular complications (6, 25). Despite lower basal HR (HR in Fig. 2A), the augmented SV in STZ-diabetic rats (SV in Fig. 2C) may cause an increase in blood flow (CO in Fig. 2B) and maintain blood pressure as seen in age-matched controls (Table I). Reserves in Frank-Starling operation may account for the compensatory stroke volume and then for the maintenance of arterial blood pressure (26). These hemodynamic changes by diabetes in male rats are in accordance with many other reports in the literature (8, 9, 25). Although there was a trend toward increasing CO and SV and decreasing total peripheral resistance, the differences were not significant in female rats with insulin deficiency.

To aortic distensibility of STZ-diabetic rats of either gender, the physiological implication of reduced Z_c (Z_c in Fig. 3A) seems to conflict with that of diminished τ (τ in Fig. 4D). Decreased aortic characteristic impedance may be indicative of more distensible aortas, whereas diminished wave transit time may have an opposite physical meaning. With unaltered aortic pressure, a decline in aortic characteristic impedance suggests that the contractile function of the vascular smooth muscle cells may be impaired in Windkessel vessel (4). Under isobaric vasodilatation, the inacti-

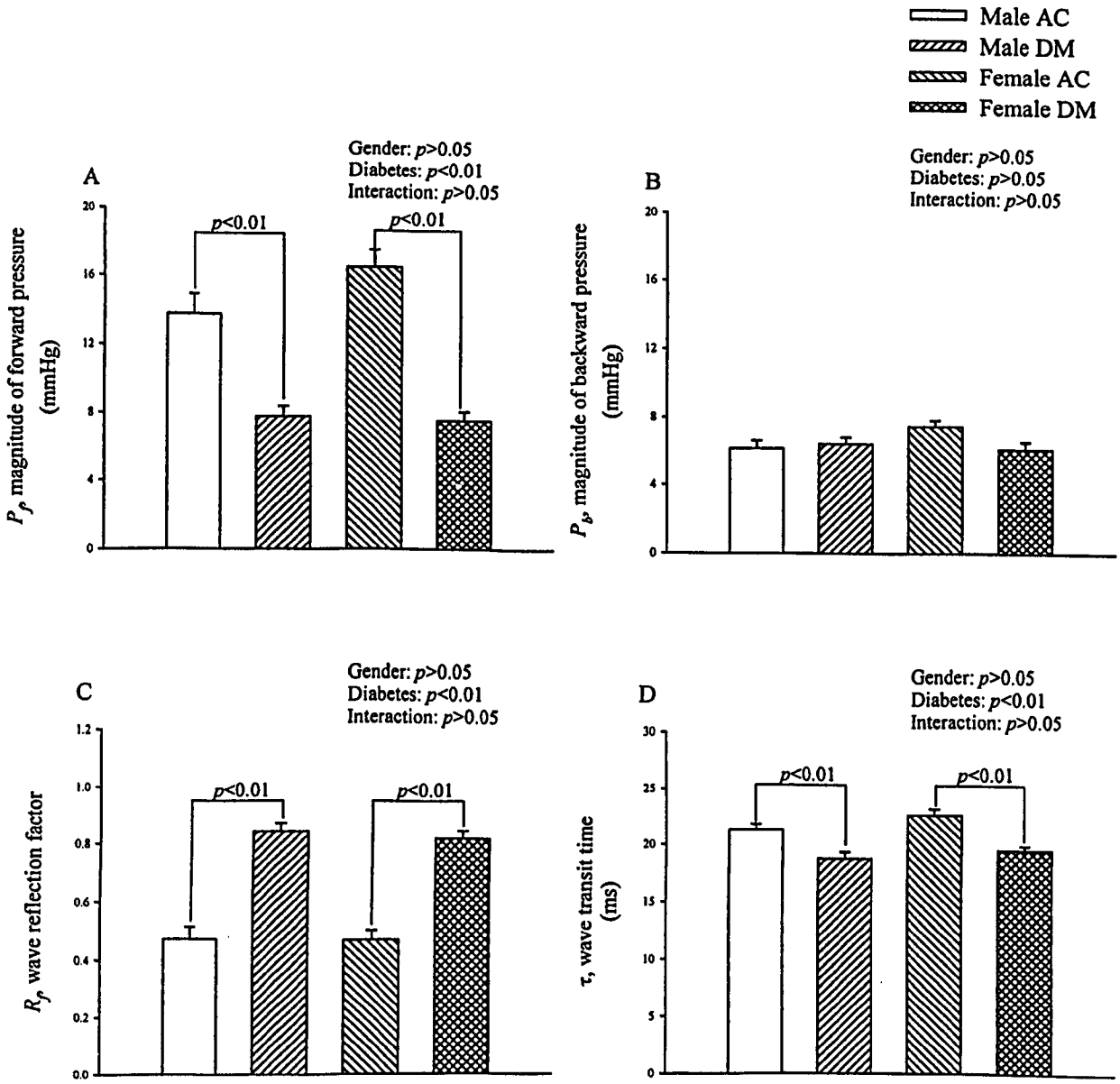

Figure 4. Effects of diabetes and gender on magnitude of the P_f (A), magnitude of the P_b (B), R_f (C), and τ (D). AC, age-matched controls; DM, STZ-diabetic rats.

vation of the aortic smooth muscle cells has the potential to elevate the elastic modulus of the aortic wall and cause a fall in aortic distensibility (11). Meanwhile, the contractile dysfunction of the diabetic aortas probably lengthens the aortic smooth muscle cells, resulting in an increase in aortic lumen diameter that can cause a fall in aortic characteristic impedance. Because the net results of diabetes and gender on the aortic characteristic impedance would depend on the relative influence of those counter-balancing factors, i.e., pulse wave velocity and aortic cross-sectional area, there is difficulty using the aortic characteristic impedance to describe the aortic distensibility in male or female STZ-diabetic rats.

As mentioned earlier, a decline in aortic distensibility could be reflected in the reduction in wave transmission time along the path. STZ-diabetic rats of either gender did show a decline in wave transit time of the lower body circulation compared with controls. To rule out the influence of body shape on wave transit time, comparison was also made between diabetic rats and weight-matched controls, and STZ-diabetic rats of either gender still exhibited shorter wave transit time of the body circulation (18.82 ± 0.60 vs 20.95 ± 0.43 msec in males; 19.63 ± 0.37 vs 22.22 ± 0.31 msec in females). As a consequence, the decreased aortic distensibility in both male and female STZ-diabetic rats may be manifest on the reduced wave transit time rather than on the diminished aortic characteristic impedance. The increased stiffness of aortic wall found in STZ-diabetic rats is in accordance with those observed in humans with type 1 diabetes (27). Because we have no measurements on aortic lumen diameter, more studies are needed to delineate the effects of isobaric vasodilatation on aortic distensibility in male or female STZ-diabetic rats.

Just as the elastic modulus is an expression used to characterize the material properties, so distensibility is a term used to describe the elastic behavior of a hollow vessel or chamber. As mentioned earlier, compliance and distensibility are quite different, for compliance is equal to distensibility times volume (15). In the present study, no significant changes in aortic compliance were observed in female STZ-diabetic rats, whereas male STZ-diabetic rats did show an increase in this hemodynamic parameter (Fig. 3, B–D). The decreased aortic distensibility associated with unchanged (in females) or increased (in males) aortic compliance suggests that volume expansion in the arterial system may exist in both male and female STZ-diabetic rats. The volume expansion in STZ-diabetic rats is supported by other reports in the literature (6, 28).

As mentioned earlier, the wave transit time is the time for a wave to propagate from one end of the vasculature to the other. The shorter τ observed in both male and female STZ-diabetic rats (τ in Fig. 4D) suggests that diabetes may cause an early return of pulse wave reflection from the peripheral circulation. Meanwhile, diabetes contributed to a significant fall in magnitude of the P_f (P_f in Fig. 4A), whereas the magnitude of the P_b remained unchanged (P_b in Fig. 4B). The reduced P_f by diabetes associated with the unaltered P_b was responsible for the augmented R_f (R_f in Fig. 4C) in both male and female STZ-treated rats. The enhanced R_f is indicative of the heavy reflection intensity in the arterial system. Thus, changes in τ and R_f suggest that diabetes may modify the timing and magnitude of the pulse wave reflection in the vasculature from both male and female STZ-treated rats.

Abnormality of blood viscosity may play a role in the underlying mechanism of the development of diabetic complications. The whole blood viscosity had been reported to be a dichotomy response to STZ-induced diabetes, depending on hematocrit and shear rate (29). Having no measurements on blood viscosity, we cannot reach any conclusions about the effects of blood viscosity on the aortic input impedance in STZ-diabetic rats of either gender. More studies are needed to delineate how the viscosity of blood affects the aortic input impedance measured in STZ-diabetic rats.

Reportedly, STZ is an antibiotic that is selectively toxic for pancreatic β cells and can cause DM in the rat (30). The diabetogenic effects of STZ are found to be dose dependent, and dose of 65 mg/kg is used in most cardiovascular studies (31). Rats treated with STZ display many of the features as seen in human subjects with uncontrolled DM, including hyperglycemia, polydipsia, polyuria, and weight loss (32). However, STZ has the potential to affect many factors such as endocrine, renal, hepatic, nervous, cardiac, and vascular factors that may underlie changes in cardiovascular homeostasis. The results reported here were obtained in STZ-diabetic rats and caution should be noted in extrapolating all findings from STZ-diabetic rats to human subjects with insulin deficiency.

Because the aortic input impedance cannot be measured in conscious animals, it is difficult to evaluate the effects of pentobarbital anesthesia on STZ-diabetic rats. In this report, the results pertained only to measurements made in the anesthetized open-chest rat. This setting induced a fall in blood pressure and may introduce reflex effects not found in the closed-chest setting (13). It is uncertain how great the effects of anesthesia and thoractomy are on the arterial mechanics in rats. However, studies with other animal models suggest that the effects are small relative to the biological and experimental variability between animals (16).

In summary, we determined the effects of diabetes and gender on the arterial mechanics in STZ-treated rats based on the aortic input impedance analysis. Only in male rats does diabetes produce a detriment in the physical properties of the resistance arterioles, causing a decline in total peripheral resistance. However, despite gender, diabetes diminishes the aortic distensibility and impairs the pulse wave reflection in rats with insulin deficiency. Unlike STZ-diabetic rats, age-matched controls show no gender-related differences in arteriolar function and pulsatile nature of blood flows in arteries.

1. The Diabetes Control and Complications Trial Research Group. The effect of intensive treatment of diabetes on the development and progression of long-term complications in insulin-dependent diabetes mellitus. N Engl J Med **329**:977–986, 1993.
2. Garcia MJ, McNamara PM, Gordon T, Kannel WB. Morbidity and mortality in diabetics in the Framingham population. Sixteen-year follow-up study. Diabetes **23**:105–111, 1974.
3. Barrett-Connor E, Bush TL. Estrogen and coronary heart disease in women. J Am Med Assoc **265**:1861–1867, 1991.
4. Williamson JR, Chang K, Tilton RG, Kilo C. Models for studying diabetic complications. In: Creutzfeldt W, Lefebvre P, Eds. Diabetes Mellitus: Pathophysiology and Therapy. New York: Springer-Verlag, pp142–151, 1989.
5. Letwin SE, Raya TE, Daugherty S, Goldman S. Peripheral circulatory control of cardiac output in diabetic rats. Am J Physio **261**(Heart Circ Physiol 30):H836–H842, 1991.
6. Zatz R, Brenner BM. Pathogenesis of diabetic microangiopathy: the hemodynamic view. Am J Med **80**:443–453, 1986.
7. Penpargkul S, Fein F, Sonnenblick EH, Scheuer J. Depressed sarcoplasmic reticular function for diabetic rats. J Mol Cell Cardiol **13**:303–309, 1981.
8. Carbonell LF, Salom MG, Garcia-Estan J, Salazer FJ, Ubeda M, Quesada T. Hemodynamic alterations in chronically conscious unrestrained diabetic rats. Am J Physiol **252**(Heart Circ Physiol 21):H900–H905, 1987.
9. Chang KC, Chen TJ, Peng YI, Li TH, Tseng YZ. Impaired vascular dynamics in normotensive diabetic rats induced by streptozotocin: tapered T-tube model analysis. J Theor Biol **204**:371–380, 2000.
10. McDonald DA. Blood Flow in Arteries. London: Arnold, 1974.
11. Milnor WR. Hemodynamics. Baltimore: Williams & Wilkins, 1989.
12. Nichols WW, O'Rourke MF. McDonald's Blood Flow in Arteries. London: Arnold, 1998.
13. Zuckerman BD, Yin FCP. Aortic impedance and compliance in hypertensive rats. Am J Physiol **257**:H553–H562, 1989.
14. Chang KC, Tseng YZ, Huo TS, Chen HI. Impaired left ventricular relaxation and arterial stiffness in patients with essential hypertension. Clin Sci **87**:641–647, 1994.
15. Guyton AC. Human Physiology and Mechanisms of Disease. Philadelphia: Saunders, 1992.

16. Cox RH. Three-dimensional mechanics of arterial segments in vitro methods. J Appl Physiol **36**:381–384, 1974.
17. Huijberts MS, Wolffenbuttel BH, Boudier HA, Crijns FR, Kruseman AC, Poitevin P, Lévy BI. Aminoguanidine treatment increases elasticity and decreases fluid filtration of large arteries from diabetic rats. J Clin Invest **92**:1407–1411, 1993.
18. Gaballa MA, Raya TE, Hoover CA, Goldman S. Effects of endothelial and inducible nitric oxide synthases inhibition on circulatory function in rats after myocardial infarction. Cardiovasc Res **42**:627–635, 1999.
19. Laxminarayan S, Sipkema P, Westerhof N. Characterization of the arterial system in the time domain. IEEE Trans Biomed Eng **25**:177–184, 1978.
20. Mitchell GF, Pfeffer MA, Westerhof N, Pfeffer JM. Measurement of aortic input impedance in rats. Am J Physiol **267**(Heart Circ Physiol 36):H1907–H1915, 1994.
21. Liu A, Brin KP, Yin FCP. Estimation of total arterial compliance: an improved method and evaluation of current methods. Am J Physiol **251**(Heart Circ Physiol 20):H588–H600, 1986.
22. Sipkema P, Westerhof N, Randall OS. The arterial system characterized in the time domain. Cardiovasc Res **14**:270–279, 1980.
23. Latson TW, Yin FCP, Hunter WC. The effects of finite wave velocity and discrete reflection on ventricular loading. In: Yin FCP, Ed. Ventricular/Vascular Coupling. New York: Springer-Verlag, pp354–383, 1987.
24. Westerhof N, Sipkema P, VanDen Bos GC, Elzinga G. Forward and backward waves in the arterial system. Cardiovasc Res **6**:648–656, 1972.
25. Parving HH, Viberti GC, Keen H, Christiansen JS, Lassen NA. Hemodynamic factors in the genesis of diabetic microangiopathy. Metabolism **32**:943–949, 1983.
26. Peng YI, Chang KC. Acute effects of methoxamine on left ventricular-arterial coupling in streptozotocin-diabetic rats: a pressure-volume analysis. Can J Physiol Pharm **78**:415–422, 2000.
27. Wilkinson IB, MacCallum H, Rooijmans DF, Murray GD, Cockroft JR, McKnight JA, Webb DJ. Increased augmentation index and systolic stress in type 1 diabetes mellitus. QJM **93**:441–448, 2000.
28. Tomlinson KC, Gardiner SM, Hebden RA, Bennett T. Functional consequences of streptozotocin-induced diabetes mellitus, with particular reference to the cardiovascular system. Pharmacol Rev **44**:103–150, 1992.
29. Nukada H, Simpson LO, Robertson AM. Dichotomous response of whole blood viscosity in streptozotocin-diabetic rats. Diabetes Res **22**:21–32, 1993.
30. Rakieten N, Rakieten ML, Nadkarni MV. Studies on the diabetogenic action of streptozotocin. Cancer Chemother Rep **29**:91–98, 1963.
31. Junod A, Lambert AE, Stauffacher W, Renold AE. Diabetogenic action of streptozotocin: relationship of dose to metabolic response. J Clin Invest **48**:2129–2139, 1969.
32. Tomlinson KC, Gardiner SM, Bennett T. Diabetes mellitus in Brattleboro rats: cardiovascular, fluid, and electrolyte status. Am J Physiol **256**:R1279–R1285, 1989.

Appendix 1

Impedance analysis using a standard Fourier series expansion technique. The aortic pressure and flow signals are subjected to Fourier transform to obtain the pressure and the flow harmonics (10–12):

$$p(k) = \sum_{n=0}^{N-1} P(n)\omega_N^{kn} \quad (1)$$

$$q(k) = \sum_{n=0}^{N-1} Q(n)\omega_N^{kn} \quad (2)$$

where $k = 0, 1, 2, 3, \ldots, N-1$; $P(n)$ is the sampled sequence of measured pressure wave; $Q(n)$ the sampled sequence of measured flow wave; $p(k)$ the complex function of pressure at k^{th} harmonic; $q(k)$ the complex function of flow at k^{th} harmonic; $\omega_N = e^{-j2\pi/N}$ and $j = \sqrt{-1}$. $p(k)$ and $q(k)$ can be rewritten as:

$$p(k) = |p(k)|e^{j\phi(k)} \quad (3)$$

$$q(k) = |q(k)|e^{j\varphi(k)} \quad (4)$$

For k^{th} sinusoidal signal, the aortic input impedance $z(k)$ is the ratio of ascending aortic pressure harmonic to the corresponding flow harmonic:

$$z(k) = \frac{p(k)}{q(k)} = \frac{|p(k)|e^{j\phi(k)}}{|q(k)|e^{j\varphi(k)}} = \frac{|p(k)|}{|q(k)|}e^{j[\phi(k)-\varphi(k)]} \quad (5)$$

where $|z(k)| = |p(k)|/|q(k)|$ is the modulus and $\vartheta(k) = \phi(k) - \varphi(k)$ is the phase of the impedance. The level of the flow noise is determined by Fourier analysis of the middle third of the diastolic flow signal (13). Any flow harmonic with a modulus <1.5 times the noise level is not used for impedance calculation.

Appendix 2

Exponential pressure-volume relationship in arteries. Because of a curvilinear relation between pressure and intravascular volume in the arterial tree, the arterial compliance C at any pressure P is obtained from the equation developed for an exponential pressure-volume relationship (21):

$$C(P) = \frac{SV \times b}{K + Z_c \times SV/A_d} \times \frac{e^{b\times P}}{e^{b\times P_i} - e^{b\times P_d}} \quad (1)$$

where SV is the stroke volume; K is the ratio of total area under the aortic pressure curve to the diastolic area (A_d); b is the coefficient in the pressure-volume relation (-0.0131 ± 0.009 in aortic arch); P_i is the pressure at the time of incisura and P_d is the end-diastolic pressure.

Appendix 3

Arterial wave reflection phenomenon. The aortic pressure and flow waves can be separated into their forward and backward components by the method Westerhof *et al.* proposed (24). In the time domain, the following mathematical formulation is the technique used to decompose the measured waves into their forward and backward components, assuming that Z_c is a real number.

$$P_f = (P + Z_cQ)/2 \quad (1)$$

$$P_b = (P - Z_cQ)/2 \quad (2)$$

$$Q_f = (Z_cQ + P)/2Z_c \quad (3)$$

$$Q_b = (Z_cQ - P)/2Z_c \quad (4)$$

P is the measured aortic pressure and Q is the measured aortic flow, and subscripts f and b represent forward and backward, respectively. The time domain reflection factor (R_f) can be derived as the amplitude ratio of backward-to-forward peak pressure wave. Therefore, both the wave transit time and the wave reflection factor characterize the wave reflection phenomenon in the arterial system.